Effect of the Polydispersity of Molecular Length on the Decay Process of Transient Electric Birefringence of Rodlike Macromolecules in Dilute Solution

Kiwamu YAMAOKA* and Kiyohiro FUKUDOME

Faculty of Science, Hiroshima University, Higashisenda-machi, Naka-ku, Hiroshima 730

(Received July 2, 1982)

The effect of polydispersity on transient electric birefringence (EB) was examined for a dilute solution which contains like macromolecules of varying lengths. The molecules were assumed to be rigid rods of cylindrical symmetry, so that the molecular weight is linearly proportional to length. Polydispersity was expressed by the ratio of the weight-average to the number-average lengths l_w/l_n. A logarithmic-normal type continuous length distribution was generally used. Calculations were performed for the birefringence-average relaxation time $\langle\tau\rangle_{EB}$ and initial slope $\langle S\rangle_{EB}$ as a function of the electric field strength E, which is applied prior to the start of the decay process, with the electric parameter $(\beta_w)^2/2\gamma_w$, which is related to the weight-average permanent dipole moment (the β_w-term) and polarizability anisotropy (the γ_w-term). Both $\langle\tau\rangle_{EB}$ and $\langle S\rangle_{EB}$ are very sensitive to E, l_w/l_n, and $(\beta_w)^2/2\gamma_w$. A convenient method was devised for determining the polydispersity parameters (l_w/l_n and l_w) from the weight-averages of relaxation time and initial slope, which are free from the mechanism of field orientation. Examples are given for a polydisperse, rigid rodlike sonicated DNA sample in aqueous solution.

In the preceding paper on the electric birefringence (EB) and electric dichroism (ED) of sonicated DNA in dilute solutions,[1] we have indicated that the measurement of decay processes is promising for determining the overall molecular shape, even if the sample DNA is polydisperse as regards the molecular length. Although the theoretical basis of the transient EB and ED methods is well advanced for monodisperse systems,[2] analyses of the experimental data of a polydisperse system have often been unsatisfactory because of the lack of an appropriate procedure. For a polydisperse system consisting of particles with a continuous length distribution, Yoshioka and Watanabe[3,4] first introduced the area method, by which the electric birefringence-average relaxation time, $\langle\tau\rangle_{EB}$, can be obtained. They have since developed an elegant method for determining the relaxation spectrum from a single decay curve.[5–11] According to our experience, the application of this method to dilute polymer solutions is often difficult due to low signal-to-noise ratio of observed decay signals. Kobayasi has calculated the variation of relaxation time τ with the polydispersity ratio of a continuous weight distribution for rodlike molecules.[12] Schweitzer and Jennings have shown that the initial slope, S, of a decay curve depends not only on the particle-size distribution and electric field strength, but also on the nature of the electric properties of molecules.[13,14] Coles and Weill have discussed the relation between the initial slopes and various averages of rotary diffusion coefficients.[15]

The objective of this paper is to clarify the effect of the molecular length distribution on the electro-optical and hydrodynamic properties of polydisperse samples and to allow the evaluation of the degree of polydispersity, which is defined as the weight-average to the number-average lengths l_w/l_n, and of the weight-average length l_w from the observed decay data. For this purpose, we first calculate the values of $\langle\tau\rangle_{EB}$ and $\langle S\rangle_{EB}$ numerically for an assembly of nonionized and rodlike dipolar macromolecules, showing the dependence of these values on externally applied electric field strength. We secondly discuss the use of a newly devised "mesh method" for evaluating both l_w/l_n and l_w by applying it to the actually observed relaxation data of a polydisperse, rigid rodlike sonicated DNA sample.[1]

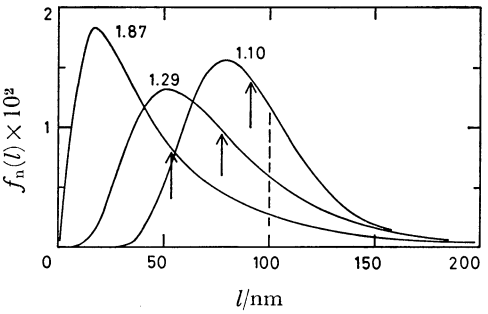

Fig. 1. The logarithmic-normal function $f_n(l)$ for continuous length distribution with various ratios of l_w/l_n. The weight-average length l_w is assumed to be 100 nm in all cases, as indicated by a vertical line. The positions of the number-average length l_n are indicated by arrows. Numerals denote the polydispersity ratio l_w/l_n.

Formalism and Calculations

Continuous Length Distribution. The following assumptions are made. A macromolecular species in a given polydisperse system is a thin, rigid rod of cylindrical symmetry with the longitudinal length l, having the apparent electric permanent dipole moment along the symmetry axis (the 3-axis), μ, and the electric polarizability anisotropy, $\Delta\alpha=(\alpha_{33}-\alpha_{11})$.[16–18] The density and the optical properties of molecules in the system are independent of molecular lengths. Both μ and $\Delta\alpha$ are proportional to l, so that $\mu=\mu_0 l$ and $\Delta\alpha=\Delta\alpha_0 l$, where μ_0 and $\Delta\alpha_0$ are the respective quantities per unit length.[19] The probability density function of l is $f_n(l)$ on the basis of the number of molecules in a solution. For $f_n(l)$, we mostly use a logarithmic-normal distribution, *i.e.*, the Wesslau function (Eq. 1),[20] in order to emphasize the contribution from fewer but longer components. (We have also examined the Schulz-Zimm,[1] the Poisson, and a rectangular distribution function.

The results are qualitatively all the same.)

$$f_n(l) = \frac{l_L}{l^2\omega\sqrt{\pi}\exp\left(\frac{\omega^2}{4}\right)}\exp\left\{-\frac{1}{\omega^2}\left(\ln\frac{l}{l_L}\right)^2\right\}, \quad (1)$$

where l_L is the parameter which determines the absolute position of the distribution and ω is the parameter which determines its breadth. The ratio $l_w/l_n = \exp(\omega^2/2)$, $l_n = l_L\exp(-\omega^2/4)$, and $l_w = l_L\exp(\omega^2/4)$. Figure 1 shows $f_n(l)$ with three different values of l_w/l_n.

Field-strength Dependence of EB Decay Processes. For a polydisperse system, the birefringence-average relaxation time $\langle\tau\rangle_{EB}$ (the same type expressions are also applicable to ED) can be expressed as follows:[3,12,21]

$$\langle\tau\rangle_{EB} = \int_0^\infty \frac{\Delta n(t)}{\Delta n(0)}dt = \frac{\int_a^{a'}\tau(l)\Phi(\beta',\gamma')lf_n(l)dl}{\int_a^{a'}\Phi(\beta',\gamma')lf_n(l)dl}, \quad (2)$$

where $\Delta n(0)$ is the steady-state birefringence at the initial time ($t=0$) when an electric pulse of arbitrary field strength is removed, and $\tau(l)$ is the relaxation time of a component with a length of l. The initial slope is given as[13–15]

$$\langle S\rangle_{EB} = \left[\frac{d\left(\ln\frac{\Delta n(t)}{\Delta n(0)}\right)}{dt}\right]_{t\to 0} = -\left\langle\frac{1}{\tau}\right\rangle_{EB}$$

$$= -\frac{\int_a^{a'}\tau(l)^{-1}\Phi(\beta',\gamma')lf_n(l)dl}{\int_a^{a'}\Phi(\beta',\gamma')lf_n(l)dl}, \quad (3)$$

where $\beta' = \mu_0 lE/kT$ and $\gamma' = \Delta\alpha_0 lE^2/2kT$. Since the orientation function $\Phi(\beta',\gamma')$ approaches unity, as the field strength increases infinitely, both $\langle\tau\rangle_{EB}$ and $\langle S\rangle_{EB}$ at infinitely high field give the weight-average relaxation time $\langle\tau\rangle_w$ and the weight-average initial slope $\langle S\rangle_w$, respectively:

$$\langle\tau\rangle_w = \frac{\int_a^{a'}\tau(l)lf_n(l)dl}{\int_a^{a'}lf_n(l)dl}, \quad (4)$$

and

$$\langle S\rangle_w = -\frac{\int_a^{a'}\tau(l)^{-1}lf_n(l)dl}{\int_a^{a'}lf_n(l)dl}. \quad (5)$$

It should be emphasized that neither $\langle\tau\rangle_w$ nor $\langle S\rangle_w$ depends on the electric properties (β' and γ') and hence, not on the orientation mechanism. The relaxation time $\tau(l)$ for a thin, rodlike molecule of length l may be calculated from several expressions.[2] We employ the Broersma equation[22] (*cf.* Eq. 8 in Ref. 1).

In actual computations for $\Phi(\beta',\gamma')$, $\langle\tau\rangle_{EB}$, and $\langle S\rangle_{EB}$ as a function of electric field strength, the following values were used, unless otherwise specified:

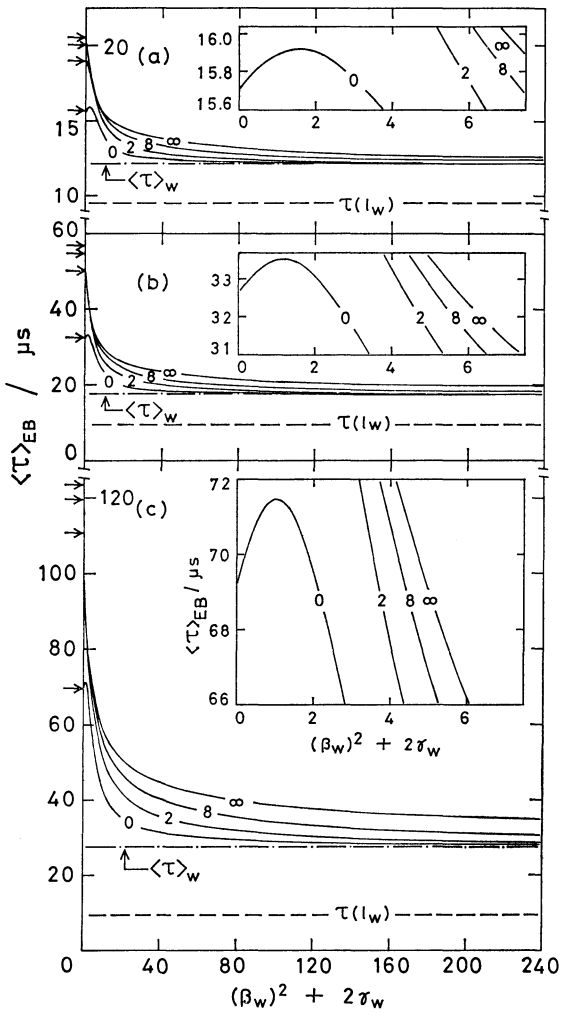

Fig. 2. Electric birefringence-average relaxation time $\langle\tau\rangle_{EB}$ as a function of $[(\beta_w)^2+2\gamma_w]$ for the polydisperse system with the l_w/l_n ratios of (a) 1.10, (b) 1.29, and (c) 1.87. Numerals in each figure correspond to the values of $(\beta_w)^2/2\gamma_w$; polarizability anisotropy only (0), mixed dipole (2 and 8), and permanent dipole only (∞). Lateral arrows on the ordinates indicate values of $\langle\tau\rangle_{EB}$ at limiting low fields. In each figure, the weight-average relaxation time $\langle\tau\rangle_w$ is shown by (—·—), while the field-independent relaxation time $\tau(l_w)$ for a monodisperse system, in which the length $l_w(=l_0)$ is 100 nm, is shown by (----). Inserts are the plots of $\langle\tau\rangle_{EB}$ *vs.* $[(\beta_w)^2+2\gamma_w]$ in the low field region. Note the scale on the ordinate of (a) differs from that of (b) and (c).

$\mu_0 = 3.0\times10^{-19}$ C (or 8.993 D/Å), $\Delta\alpha_0 = 1\times10^{-25}$ F m (or 8.985×10^{-12} cm^2) for the pure anisotropy orientation ($\Delta\alpha$ is variable for the mixed dipole orientation[17,18]), $l_w = 100$ nm, $2b$ (the diameter of a cylinder) $= 1.5$ nm, the viscosity of solvent $\eta_0 = 8.45\times10^{-4}$ Pa s, and $T = 293$ K. The upper and lower integral limits are set as $a = 5$ nm and $a' = 405$ nm, rather than as $a = 0$ and $a' = \infty$, because low molecular-weight-oligomers are often removed from a polymer sample (the upper limit was set for the convenience of completing computations with a sufficient accuracy).

Results and Discussion

Effect of Polydispersity on Relaxation Time. The field-strength dependence of $\langle\tau\rangle_{EB}$, calculated from Eq. 2, is plotted in Fig. 2 against $[(\beta_w)^2+2\gamma_w]$ at several ratios of $(\beta_w)^2/2\gamma_w$, where β_w and γ_w are the weight-averages of β' and γ'. The weight-average relaxation time $\langle\tau\rangle_w$ is drawn in each figure by a dash-dotted line, together with the field-independent single relaxation time $\tau(l_w)$ for the corresponding monodisperse system with the length of $l_o(=l_w)$ (dashed line) for comparison. The results are summarized below. (1) The relaxation time of a given polydisperse system strikingly depends on the electric pulse field applied prior to the start of decay process. This field dependence is quite sensitive to the polydispersity of the sample; hence, it is the best test for a length distribution. (2) The magnitude of $\langle\tau\rangle_{EB}$ is exceedingly large at extremely low electric field, as the ratio l_w/l_n increases. For example, the value of $\langle\tau\rangle_{EB}$ is as high as 123 μs for the most polydisperse sample ($l_w/l_n=1.87$), while it is only 9.62 μs for the corresponding monodisperse system (Fig. 2(c)). This is because $\tau(l)$ is proportional to the cube of l and because the polydisperse sample contains the components whose lengths are much longer than l_w (*cf.* Fig. 1). (3) In each polydisperse system, values of $\langle\tau\rangle_{EB}$ rapidly decrease with increasing field strengths and gradually become level. They should all approach the limiting value, *i.e.*, $\langle\tau\rangle_w$, which depends only on polydispersity and length.[12,17] (4) The field-strength dependence of $\langle\tau\rangle_{EB}$ is characteristic of the orientation mechanism. The pure permanent dipole moment orientation clearly shows a large but monotonous dependence. For pure polarizability orientation, however, the field dependence is not monotonous. In the low field range, there appears a maximum whose magnitude and position depend on polydispersity (see inserts in Figs. 2(a)—(c)). (5) For any polydisperse system, $\langle\tau\rangle_w$ does not coincide with $\tau(l_w)$, unless the length distribution is extremely narrow. This is an important consequence of polydispersity. If an average length of solutes in a polydisperse sample is calculated directly from the Broersma equation by using the experimentally obtained relaxation time $\langle\tau\rangle_w$ or $\langle\tau\rangle_{EB}$, the length would be unreasonably large. (It is $\tau(l_w)$ that is related to the weight-average length l_w.) Hence, an erroneous conclusion may be drawn on the overall solution conformation of the polymer system in which molecular lengths are heterogeneous.

Effect of Polydispersity on Initial Slope. The initial slope $\langle S\rangle_{EB}$ of a decay signal is a measure of polydispersity.[8,9,13,14] The results of the present calculation are illustrated in Fig. 3. Values of $\langle S\rangle_{EB}$ clearly depend on polydispersity ratio and field-orientation mechanism, slowly approaching the weight-average $\langle S\rangle_w$ at limiting high fields, which is, however, independent of the orientation mechanism in a manner similar to the case of relaxation time. It is interesting to note that values of $\langle S\rangle_{EB}$ in the low field range are close to the value of $S(l_w)$ for the monodisperse

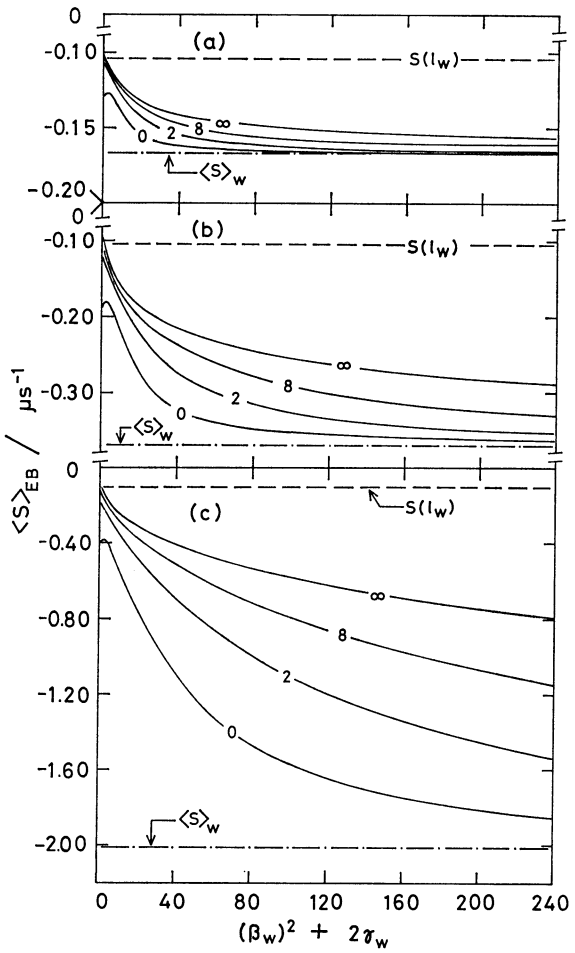

Fig. 3. Electric birefringence-average initial slope $\langle S\rangle_{EB}$ as a function of $[(\beta_w)^2+2\gamma_w]$ for a polydisperse system with three l_w/l_n ratios of (a) 1.10, (b) 1.29, and (c) 1.87. In each figure, the weight-average initial slope $\langle S\rangle_w$ is given by (—·—) and the field-independent initial slope $S(l_w)$ for a monodisperse system by (----), in which the length ($l_w=l_o$) is 100 nm.

system (dashed line), if solutes are oriented predominantly by the permanent dipole moment $[(\beta_w)^2/2\gamma_w=\infty$—8]. For pure polarizability orientation, an extremum appears in the low field range, similarly to the case of the corresponding relaxation time.

Estimation of Weight-average Relaxation Time and Initial Slope. Values of $\langle\tau\rangle_w$ and $\langle S\rangle_w$ can be estimated by extrapolation of those of $\langle\tau\rangle_{EB}$ and $\langle S\rangle_{EB}$ to infinitely high field strength ($E\to\infty$). Figure 4 illustrates this extrapolation procedure with a polydisperse system ($l_w/l_n=1.29$ and $l_w=100$ nm). A problem is associated with the unknown curvature of the plot of $\langle\tau\rangle_{EB}$ or $\langle S\rangle_{EB}$ against the reciprocal of field strength. When $\langle\tau\rangle_{EB}$ is plotted against $[(\beta_w)^2+2\gamma_w]^{-1}$, which is proportional to E^{-2} (Fig. 4(a)), the curvature is convex and quite large for the permanent dipole moment orientation (∞), but it becomes concave with decreasing $(\beta_w)^2/2\gamma_w$ (2 and 0). When $\langle\tau\rangle_{EB}$ is plotted against $[(\beta_w)^2+2\gamma_w]^{-1/2}$, which is proportional to E^{-1} (Fig. 4(b)), the curvature is only slightly concave for all $(\beta_w)^2/2\gamma_w$ (∞—0). The similar results with reversed curvatures are found for $\langle S\rangle_{EB}$ (dashed curves in Figs. 4(a)—(b)). These plots are suggestive of

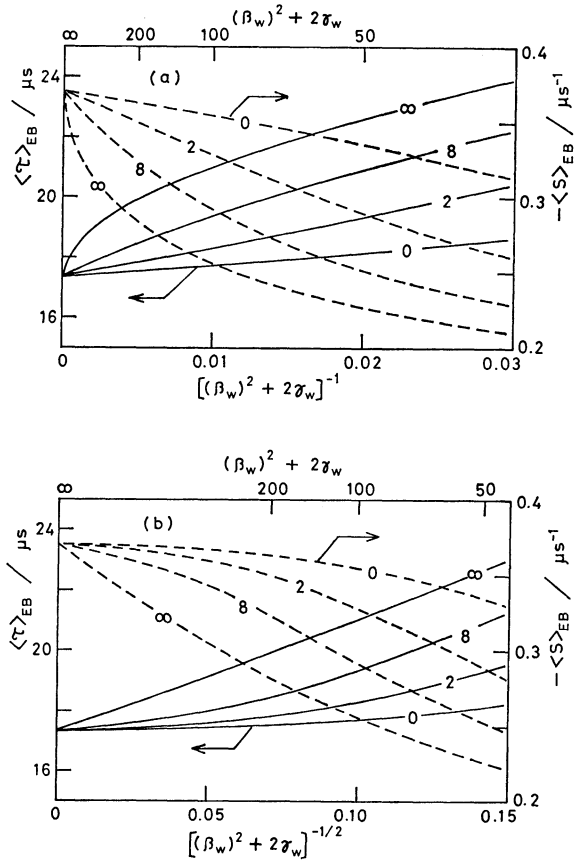

Fig. 4. Extrapolations of the birefringence-average relaxation time $\langle\tau\rangle_{EB}$ and initial slope $\langle S\rangle_{EB}$ to infinitely high electric fields. The birefringence-averages were calculated for a logarithmic-normal distribution with $l_w/l_n=1.29$ and $l_w=100$ nm. Values of $\langle\tau\rangle_{EB}$ (——) and $\langle S\rangle_{EB}$ (----) are plotted against $[(\beta_w)^2+2\gamma_w]^{-1}$ in (a) and against $[(\beta_w)^2+2\gamma_w]^{-1/2}$ in (b). A numeral in each curve is the value of $(\beta_w)^2/2\gamma_w$. Note that all curves intercept the ordinates ($\langle\tau\rangle_w=17.36$ μs and $\langle S\rangle_w=-0.37$ μs^{-1}).

the proper extrapolation procedure for evaluating $\langle\tau\rangle_w$ and $\langle S\rangle_w$. For example, extrapolation of observed values of $\langle\tau\rangle_{EB}$ to the intercept of the ordinate appears to be easier if they are plotted simultaneously against E^{-1} and against E^{-2}.

Application to Measured Decay Signals of sDNA. Figure 5 shows a typical extrapolation to infinitely high field of values of $\langle\tau\rangle_{EB}$ and $\langle S\rangle_{EB}$ which are observed for a sonicated DNA (sDNA) preparation in 0.2 mM NaCl** (the experimental details are found in Ref. 1). In the case of rodlike sDNA in aqueous solutions, the dependence of $\langle\tau\rangle_{EB}$ and $\langle S\rangle_{EB}$ on field strengths has not been fully resolved, since no appropriate counterion-induced orientation function is available as yet. Nevertheless, it has been shown that the "classical" function $\Phi(\beta',\gamma')$ can represent the birefringence and dichroism behavior of sDNA adequately over a wide range of field strength.[1,23,24] The plots in Fig. 4 are based on $\Phi(\beta',\gamma')$; thus, they are instructive as an empirical guide. Observed values of $\langle\tau\rangle_{EB}$ and $\langle S\rangle_{EB}$ for sDNA are plotted both

** 1 M=1 mol dm^{-3}.

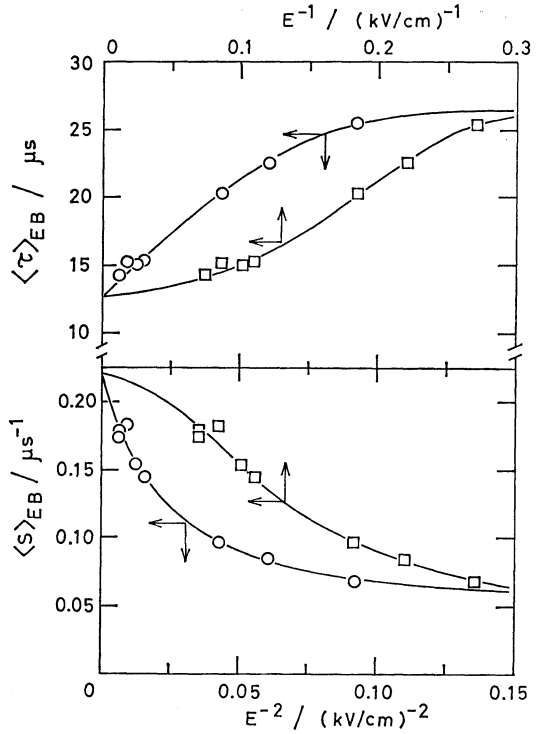

Fig. 5. Extrapolation of values of $\langle\tau\rangle_{EB}$ and $\langle S\rangle_{EB}$ experimentally obtained for a sonicated DNA sample in the 0.2 mM NaCl-containing aqueous solution.

against E^{-2} and against E^{-1} in Fig. 5. Extrapolated values are: $\langle\tau\rangle_w=12.5$ μs and $\langle S\rangle_w=-0.22$ μs^{-1}.

Evaluation of the Degree of Polydispersity and Weight-average Length. With a set of experimental values of $\langle\tau\rangle_w$ and $\langle S\rangle_w$, as obtained in the above section, both the weight-average length l_w and the polydispersity ratio l_w/l_n may be estimated, if the length distribution $f_n(l)$ is known or can be assumed for a given polydisperse system. For this purpose, we devised a new, convenient method, which may be termed the "mesh method," by constructing a theoretical graph of meshes. Examples are shown in Fig. 6, in which theoretical values of $\langle\tau\rangle_w$ (Eq. 4) are plotted against theoretical values of $\langle S\rangle_w$ (Eq. 5) with l_w and l_w/l_n as parameters. The Wesslau function (Fig. 6(a)) and the Schulz-Zimm function (Fig. 6(b))[1] are chosen for the distribution function $f_n(l)$, in order to compare the effect of the distribution curves on the final result. (The latter is said to be an appropriate function for the degradation process of chain length by sonication.[25]) Two values are assigned to 2b to see the effect of the diameter of rodlike molecules on the estimated values of l_w and l_w/l_n. A pair of experimental values ($\langle\tau\rangle_w$ and $\langle S\rangle_w$) defines a point in the $\langle\tau\rangle_w$—$\langle S\rangle_w$ coordinates; hence, the most likely set of l_w and l_w/l_n can be readily evaluated from the network. This mesh method is advantageous in that it can be used for rodlike polymers, whatever the field-orientation mechanism may be, because both $\langle\tau\rangle_w$ and $\langle S\rangle_w$ are independent of the electric parameters β' and γ' or the orientation function $\Phi(\beta',\gamma')$. The optical and electric parameters may be determined separately by the matching method previously mentioned for the steady-state birefringence[23] and dichro-

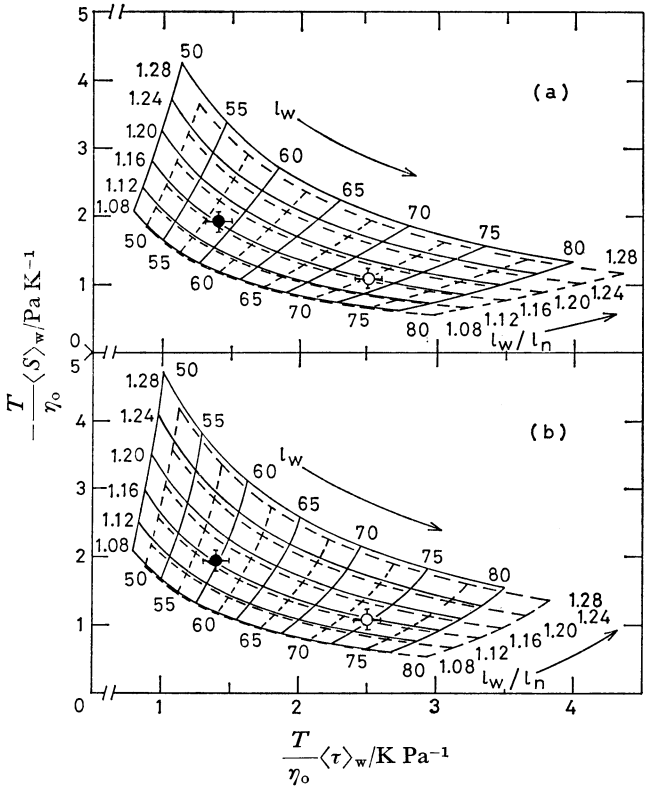

Fig. 6. The relationship between the weight-average relaxation time $\langle\tau\rangle_w$ and initial slope $\langle S\rangle_w$ with the polydispersity ratio l_w/l_n and the weight-average length l_w as the parameters. The distribution functions are the Wesslau type (a) and the Schulz-Zimm type (b). T is the absolute temperature and η_0 is the viscosity of solvent. Two different networks are plotted; one, for which the diameter of cylindrical like molecules, $2b$, is 2 nm (——), and the other with the diameter of 2.6 nm (----). For each set of meshes, values of l_w/l_n are varied between 1.08 and 1.28, while those of l_w between 50 and 80 nm. Experimental values of $\langle\tau\rangle_w$ and $\langle S\rangle_w$ for sDNA are also plotted: (○) in 0.2 mM NaCl and (●) in 0.33 mM $MgCl_2$.

ism,[24] once both l_w and l_w/l_n are available.

Paired-values of $\langle\tau\rangle_w$ and $\langle S\rangle_w$, experimentally obtained for the sDNA sample at different ionic strengths, are also plotted inside the meshes. The most probable values of l_w and l_w/l_n are summarized in Table 1. The effect of the "thickness" of a cylinder on l_w is such that the value of l_w with a diameter of 2.6 nm is smaller than that with 2.0 nm by about 5%. The choice of the distribution function is not too critical, when the range of l_w/l_n is limited to *ca.* 1.2 or less. When values of l_w are divided by the weight-average degree of polymerization or the number of base pairs (=188), the axial translation per base pair can be calculated (*cf.* Table 1 of Ref. 1). The value of l_w/l_n is close to the reported literature values (1.02—1.11),[26-28] which were determined by the sedimentation equilibrium and electron microscopic methods for fractionated sDNA samples. This good agreement, achieved by the utilization of different physical techniques and diverse sonication methods, appears to be a strong support for the present procedure for polydispersity determination.

Table 1. Polydispersity ratio, l_w/l_n, and weight-average length, l_w, of sonicated DNA in aqueous solutions evaluated by use of two distribution functions[a]

		Wesslau function		Schulz-Zimm function[b]	
	$2b$/nm[c]	2.0	2.6	2.0	2.6
A[d]	l_w/l_n	1.16	1.17	1.16	1.17
	l_w/nm	73	70	74	71
B[d]	l_w/l_n	1.16	1.17	1.16	1.17
	l_w/nm	59	56	60	57

a) The number of base pairs of this sDNA is 188.[1] b) The data are cited in Ref. 1. c) The assumed diameter of sDNA. d) sDNA in the 0.2 mM NaCl solution (A) and in the 0.33 mM $MgCl_2$ solution (B).[1]

Conclusion

With numerical calculations we could show how the decay processes of transient EB (and also ED) of a system composed of long, rigid rodlike macromolecules are affected by the polydispersity of continuous length distribution. The dependence of the relaxation time and the initial slope of an EB signal on the electric field strength applied to the system prior to the commencement of the decay is a very sensitive measure of polydispersity and field-orientation mechanism. We could show how incorrect interpretations of experimental data may be avoided. We have also described a new mesh method for determining the degree of polydispersity and the weight-average molecular length. Use of this method in conjunction with well-pursued experimental results will facilitate the EB and ED study of polydisperse, rodlike polymer systems.

References

1) K. Matsuda and K. Yamaoka, *Bull. Chem. Soc. Jpn.*, **55**, 1727 (1982).
2) "Molecular Electro-Optics, Parts 1 and 2," ed by C. T. O'Konski, Marcel Dekker, New York (1976 and 1978).
3) K. Yoshioka and H. Watanabe, *Nippon Kagaku Zasshi*, **84**, 626 (1963).
4) K. Yoshioka and H. Watanabe, "Physical Principles and Techniques of Protein Chemistry, Part A," ed by S. J. Leach, Academic Press, New York (1969), Chap. 7.
5) M. Matsumoto, H. Watanabe, and K. Yoshioka, *Biopolymers*, **6**, 929 (1968).
6) M. Matsumoto, H. Watanabe, and K. Yoshioka, *Biopolymers*, **9**, 1307 (1970).
7) M. Matsumoto, H. Watanabe, and K. Yoshioka, *Kolloid Z. Z. Polym.*, **250**, 298 (1972).
8) M. Matsumoto, H. Watanabe, and K. Yoshioka, *Biopolymers*, **11**, 1711 (1972).
9) M. Matsumoto, H. Watanabe, and K. Yoshioka, *Biopolymers*, **12**, 1729 (1973).
10) K. Tsuji, H. Watanabe, and K. Yoshioka, *Adv. Mol. Relaxation Processes*, **8**, 49 (1976).
11) K. Tsuji and H. Watanabe, *J. Colloid Interface Sci.*, **62**, 101 (1977).
12) S. Kobayashi, *Biopolymers*, **6**, 1491 (1968).
13) J. Schweitzer and B. R. Jennings, *Biopolymers*, **11**, 1077 (1972).

14) J. Schweitzer and B. R. Jennings, *Biopolymers*, **12**, 2439 (1973).
15) H. J. Coles and G. Weill, *Polymer*, **18**, 1235 (1977).
16) C. T. O'Konski and A. J. Haltner, *J. Am. Chem. Soc.*, **78**, 3604 (1956).
17) C. T. O'Konski, K. Yoshioka, and W. H. Orttung, *J. Phys. Chem.*, **63**, 1558 (1959).
18) K. Yamaoka and E. Charney, *J. Am. Chem. Soc.*, **94**, 8963 (1972).
19) P. J. Flory, "Statistical Mechanics of Chain Molecules," John Wiley & Sons, New York (1969), Chap. 9.
20) H. Wesslau, *Makromol. Chem.*, **20**, 111 (1956).
21) K. Yamaoka and K. Ueda, *J. Phys. Chem.*, **86**, 406 (1982).
22) S. Broersma, *J. Chem. Phys.*, **32**, 1626 (1960).
23) K. Yamaoka and K. Matsuda, *Macromolecules*, **14**, 595 (1981).
24) E. Charney and K. Yamaoka, *Biochemistry*, **21**, 834 (1982).
25) A. W. Davis and D. R. Phillips, *Biochem. J.*, **173**, 179 (1978).
26) G. Cohen and H. Eisenberg, *Biopolymers*, **4**, 429 (1966).
27) J. E. Godfrey, *Biophys. Chem.*, **5**, 285 (1976).
28) J. E. Godfrey and H. Eisenberg, *Biophys. Chem.*, **5**, 301 (1976).